

Mechanical behavior of TiNi shape memory alloy under axial dynamic compression

X. W. HUANG*, G. N. DONG

Theory of Lubrication and Bearing Institute, Xi'an Jiaotong University, Xi'an 710049, China
E-mail: huangxuewen@tlbi.xjtu.edu.cn

Z. R. ZHOU

Tribology Institute of Southwest Jiaotong University, Chengdu 610031, China

Y. B. XIE

Theory of Lubrication and Bearing Institute, Xi'an Jiaotong University, Xi'an 710049, China

Intermetallic compound TiNi alloys are known as shape memory alloys (SMAs) because of the thermoelastic martensitic transformation (MT) and reverse martensitic transformation. Apart from the shape memory effect (SME) [1], TiNi alloys also possess excellent pseudoelasticity (PE) [1], wear-resistance [2], corrosion-resistance [3], high damping capacity [4], good bio-compatibility [5] and outstanding mechanical properties [6]. Therefore, TiNi shape memory alloys have attracted considerable attention in recent years as functional materials in a variety of industrial and medical applications. They are called important smart materials due to their ability to perform both sensing and actuating functions [7]. A great number of investigations have been conducted on SME and PE associated with the thermoelastic martensitic transformation. Nevertheless, the transformation behavior and mechanical properties of TiNi alloys are susceptible to thermo-mechanical treatments such as cold working [8], thermal cycling [9], stress cycling [10], annealing temperature [11], aging of Ni-rich alloys [12] and addition of a third element [13]. Quite a few investigations on pseudoelasticity of TiNi alloys have been carried out by means of the tension test while the mechanical behavior under compression has not been studied. Since the materials are subjected to compression, impact as well as combinations of normal and tangent stresses in many engineering applications, it is needed to investigate, in a detailed way, the factors affecting properties of TiNi alloys under relevant conditions to extend their practical engineering applications. In this article, for the sake of simplicity, the Ni-rich Ti-50.9at% Ni alloy was selected for studying the influence of the strain rate on the mechanical behavior of TiNi alloys under axial dynamic compression and some significant results were obtained. The Ti-50.9at%Ni alloy was melted by the vacuum induction method in a graphite crucible with an argon atmosphere. The alloy ingot was homogenized at 1000 °C for 4 hr, then quenched in water. After removing the surface layer, the ingot was forged and rolled into bars of 6 mm in diameter. Before being cut into

specimens, the bars were aged at 500 °C for an hour, followed by air cooling to room temperature. The TiNi alloy bars were machined into the shape $\varnothing 5 \text{ mm} \times 14 \text{ mm}$ by wire cutting and grinding. Transformation temperatures of the alloy, which were determined by use of a differential scanning calorimeter (DSC), are given in Fig. 1. The compression experiments were conducted at 20 °C on a MTS 858Mini Bionix test machine. The experimental parameter investigated was the strain rate. The ram speeds were 3, 15, 30 and 50 mm/min, with the corresponding strain rates being about 3.571×10^{-3} , 1.786×10^{-2} , 3.571×10^{-2} and $5.952 \times 10^{-2} \text{ s}^{-1}$ respectively.

The compression stress-strain curves of Ti-50.9at%Ni alloy gained at 20 °C for various strain rates are shown in Fig. 2. It can be seen from Fig. 2a that in the case of $\dot{\epsilon} = 3.571 \times 10^{-3} \text{ s}^{-1}$, the stress increases quickly and the slope of the stress-strain curve is rather steep at the beginning, but when the stress gets to about 350 MPa, the alloy starts to “yield”, causing the stress to rise slowly and the strain to increase substantially at the same time. When unloaded at 650 MPa, the stress drops rapidly during the first stage and then the rate of

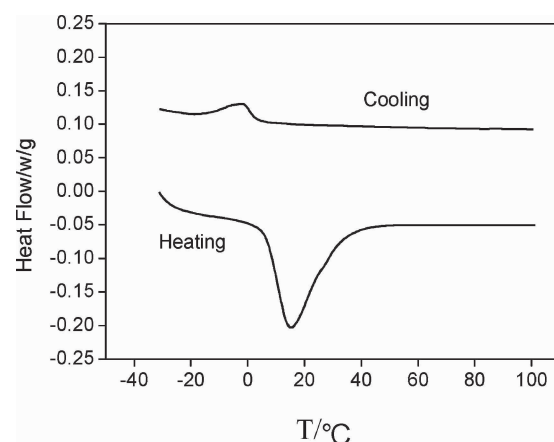


Figure 1 The DSC curve of the Ti50.9at% Ni alloy aged at 500 °C for an hour and followed by air colling.

*Author to whom all correspondence should be addressed.

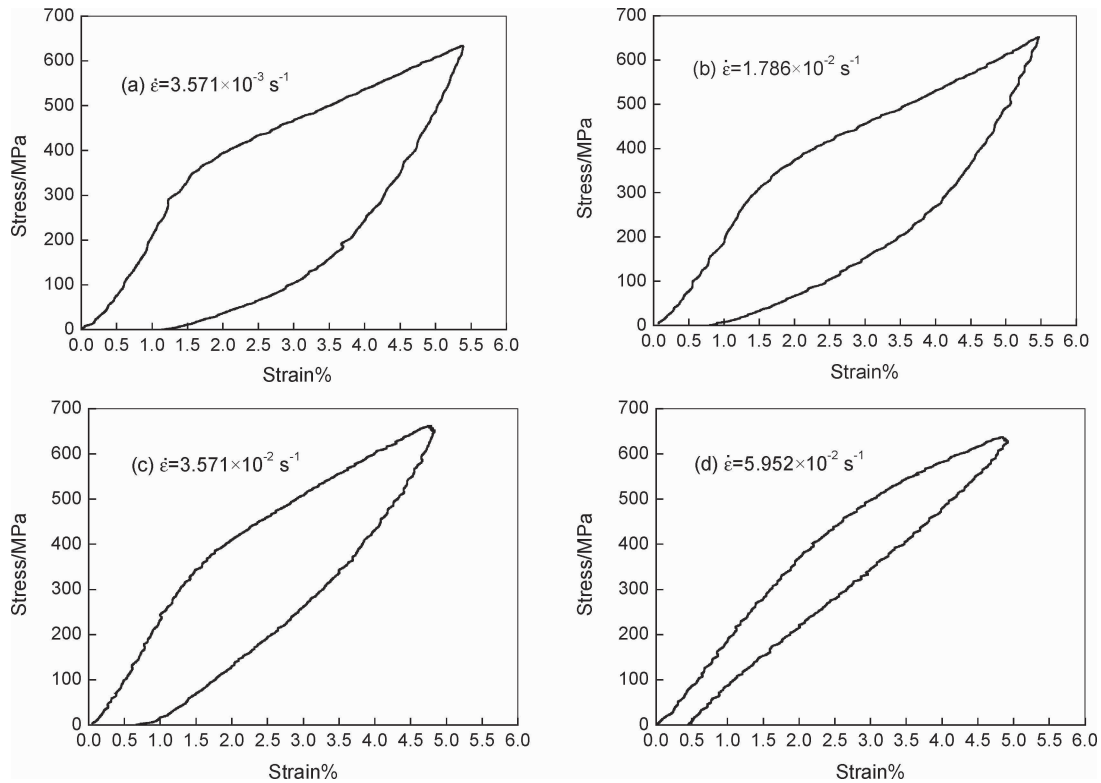


Figure 2 The influence of the strain rate on deformation characteristics of the Ti50.9at% Ni alloy at 20 °C.

decrease decelerates when the stress drops to 200 MPa. After full unloading, the strain fails to return to zero, but retains a residual strain of 1.2%. Obviously there is a fairly large stress or strain hysteresis between the loading and unloading curves. When the alloy was heated to above 40 °C, however, the residual strain disappeared and all deformation was recovered, showing the so-called shape memory effect. Since the structure of the Ti-50.9at%Ni alloy shows coexistence of parent and martensitic phases at room temperature, the elastic deformation of the parent phase and rearrangement of the martensitic phase under axial stress contributes to the strain of about 1.5% on loading. As stress increases to σ_M , i.e., the critical stress for inducing martensitic transformation, which is about 350 MPa in the case of $\dot{\epsilon} = 3.571 \times 10^{-3} \text{ s}^{-1}$, the stress-induced martensitic transformation takes place and the strain caused by this phase transformation is greatly augmented. On unloading, the reverse martensitic transformation occurs and a majority of strain is recovered as the alloy behaves pseudoelasticity. Actually the alloy also exhibits the shape memory effect because the residual strain can be recovered as the temperature increases above A_f (reverse martensitic transformation finished temperature).

As the strain rate increases, the shape of the stress-strain curve changes as displayed in Fig. 2b–d. Apparently σ_M increases and the slope of the stress-strain curve during phase transformation increases. Hence, the characteristic of transformation is not clear. Especially in the case of higher strain rate, the phase transformation plateau disappears. As indicated in Fig. 2d, the ascending tendency of the stress declines appreciably when the stress exceeds 450 MPa on loading and the relationship between the stress and strain is nearly linear on unloading. It is important to point out that the stress

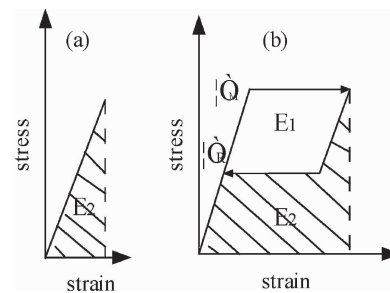


Figure 3 The schematic stress-strain curve for assessing pseudoelasticity of TiNi alloys.

or strain hysteresis decreases with the increase of the strain rate. In fact, the stress or strain hysteresis represents the material's capacity for dissipating energy. As a consequence, the damping capacity of the alloy is reduced. It is advantageous that the residual strain diminishes when the alloy exhibits the linear-like elastic deformation property at the higher strain rate.

The PE properties of TiNi alloys can be assessed using a schematic diagram such as Fig. 3, in which (a) and (b) correspond to normal materials and TiNi alloys, respectively. $E_1 + E_2$ denotes the energy absorbed per volume of material on loading; E_2 represents the stored energy density that is released on unloading, whereas E_1 is the dissipated energy density in the loading-unloading cycle resulting from the internal friction in the material. Obviously the stored energy density of TiNi alloys is much greater than that of normal materials. It is clear that with increasing strain rate, the E_2 of the Ti-50.9at%Ni alloy increases whereas E_1 decreases as shown in Fig. 2. In the case of the higher strain rate, the nonlinear pseudoelasticity, owing to phase transformation, is changed to the linear-like

pseudoelasticity. With increasing strain rate, the familiar phase transformation plateau does not appear in the stress–strain curve with smaller stress or strain hysteresis and lower damping capacity.

The influence of the strain rate on the deformation behavior of the Ti-50.9at%Ni alloy can be easily found from Fig. 2. Firstly, σ_M increases with the increase of the strain rate; secondly E2 increases and E1 declines; thirdly the stress or strain hysteresis is diminished, and then the nonlinear pseudoelasticity is transformed into the linear-like pseudoelasticity; finally the pseudoelastic strain increases with the decrease of the residual strain. This phenomenon could be attributed to strong work hardening and the microstructure of the alloy. H.C. Lin has also confirmed in his experiment that the higher the strain rate is, the greater work hardening effect exhibits [14]. The higher hardness of the alloy helps to provide an excellent pseudoelastic property because the slip is not apt to occur. However, the increase in hardness may impair the damping capacity of the alloy since the damping results from the dislocations and crystal interfaces/phase interfaces. As for the linear-like pseudoelastic deformation behavior, it can be explained in terms of the microstructure of the alloy. Since a large number of fine Ti_3Ni_4 precipitates are formed when the Ni-rich Ti-50.9at%Ni alloy is aged at 500 °C for an hour, the dispersed Ti_3Ni_4 precipitates strengthen the alloy matrix significantly. As a result, the dispersion strength effect and stress-induced martensitic transformation overlap during the deformation process and the transformation–yielding plateau is covered due to the dispersion strength effect of Ti_3Ni_4 precipitates, thus giving rise to unclear transformation characteristic. At room temperature, the Ti-50.9at%Ni alloy exhibits both pseudoelasticity (PE) and shape memory effect (SME) because this test temperature lies between A_s and A_f of the alloy and PE becomes prominent with the increase of the strain rate.

From the experimental results, the mechanical behavior characteristics of the Ti-50.9at%Ni alloy under the axial dynamic compression can be summarized as follows:

(a) At 20 °C, for $\dot{\epsilon} = 3.571 \times 10^{-3} \text{ s}^{-1}$, MT occurs when the stress reaches 350 MPa during loading and reverse MT occurs at 200 MPa during unloading. The deformation related to MT, the rearrangement of martensite and elastic strain of parent phase amounts to about 5.5% when the stress increases

to 650 MPa. The total nonlinear pseudoelastic deformation adds up to about 4.3% and a residual strain of 1.2% is retained when the stress is relieved, but the residual strain disappears when the alloy is heated above A_f , which demonstrates the shape memory effect.

(b) With increasing strain rate, σ_M increases and the transformation–yielding plateau becomes indistinct. The stress or strain hysteresis diminishes, indicating the lower damping capacity, while the stored energy density increases and the residual strain decreases.

(c) At the higher strain rate, the alloy reveals the linear-like pseudoelastic deformation behavior in the case of $\dot{\epsilon} = 5.952 \times 10^{-2} \text{ s}^{-1}$, and a linear-like pseudoelasticity of 4.5% can be obtained.

Acknowledgement

This work is supported by the National Natural Science Foundation of China (No. 50075072) and Open Foundation of Tribology Institute of Southwest Jiaotong University.

References

1. K. OTSUKA and C. M. WAYMAN, "Shape Memory Materials" (Cambridge, UK, 1998) p. 1.
2. D. Y. LI, *Wear* **221** (1998) 116.
3. T. C. ZHANG and D. Y. LI, *Mater. Sci. Eng.* **A293** (2000) 208.
4. H. C. LIN, S. K. WU and M. T. YEH, *Metal. Trans. A* **24A** (1993) 2189.
5. M. R. YANG, K. CHEN and J. LEE, *Mater. Sci. Forum* **426–432** (2003) 3055.
6. Y. F. ZHENG, W. CAI and J. X. ZHANG, *Acta Mater.* **48** (2000) 1409.
7. Z. G. WEI, C. Y. TANG and W. B. LEE, *J. Mater. Process. Technol.* **69** (1997) 68.
8. H. C. LIN and S. K. WU, *Acta Metall. Mater.* **42** (1994) 1623.
9. T. TADAKI, Y. NAKATA and K. SHIMIZU, *Trans. JIM* **28** (1987) 883.
10. J. M. GONG and T. HISAAKI, *J. Funct. Mater.* **33** (2002) 391 (in Chinese).
11. P. FILIP and K. MAZANEC, *Scr. Metall. Mater.* **32** (1995) 1375.
12. J. KHALIL ALLAFI, X. REN and E. GUNTHER, *Acta Materialia* **50** (2002) 793.
13. X. L. LU, W. CAI and L. C. ZHAO, *J. Mater. Sci. Lett.* **22** (2003) 1243.
14. H. C. LIN, H. M. LIAO and J. E. HE, *Metall. Mater. Trans. A* **28A** (1997) 1871.

Received 8 January
and accepted 1 July 2004